MAGNETOHYDRODYNAMICS Vol. 42 (2006), No. 4, pp. 451–468

CRYSTAL GROWTH IN THE PROCESS OF MODIFIED CZOCHRALSKI

F. Mokhtari[1], *A. Bouabdallah*[1], *M. Zizi*[1], *A. Alemany*[2]

[1] *Laboratory of Thermodynamics and Energetical Systems/USTHB BP32 El Alia Bab Ezzouar, Alger*

[2] *Laboratoire des Ecoulements Geophysiques et Industriels, Grenoble, France*

Basing on the phenomenon of crystal growth in a cylindrical system, one proposes an alternative of this process, which is based on the modification of the crucible. This one is replaced by a sphere containing the molten phase of possibly variable material height, the cylinder, carrying the germ of the crystal, remains unchanged. This work is thus justified by the study of the influence of the geometry for purposes to optimize the processes of transfer in action making it possible to homogenize the field of temperature and to minimize the losses of masses having to take part in the development of the bulk-flow (the traditional Czochralski process). The simulation of the phenomenon thus defined is considered in the framework of the Boussinesq approximation to solve the equations of mass, heat, and momentum transfer written in a spherical frame of reference. By means of theoritical approach as the Galerkin Method, the objective is to determine the whole process of transfer in order to optimize the fields of temperature and velocity in the alternative CZ-process.

Introduction. In the majority of the methods for the production of single crystals, the crystal is created starting from a nutritive fluid. Several mechanisms can caused flows in this fluid, which are responsible for the crystal growth because they influence the transport of the doping agent, impurity and heat towards the liquid-solid interface, which plays a major role in the process. The nutritive fluid can be a vapour or a saturated solution, but one is interested here in systems, in which the crystal grows starting from fusion.

The concept, which is at the base of the crystal growth, is simple and takes as a starting point the nature. It consists in introducing a small natural material germ in a saturated solution: a solid of ordered and defined structure reacts then with the shape of the germ and is established gradually starting from the fluid by deposit of the dissolved substance.

Although this way is simple and tempting at the same time, the first crystals obtained were, until up to now, small and relatively imperfect since they contained undesirable residual impurities and especially defects in the crystal lattice.

Currently, one is interested in a specific method of the crystal growth, the Czochralski method, considered the most significant and which is widely used. Indeed this process of growth is ideally adapted to the optimal production of great quantities of pure crystals, which are required by an increasingly demanding technology.

The variation in temperature in the system of growth is at the origin of convection in the melt. It is shown that the flows play a significant role in the process of growth while acting on the form and stability of the interface as well as on the radial distribution of the doping agents in the crystal [1].

The increase in temperature variation initiates the development of instabilities near the interface. This undesirable effect is eliminated due to to the rotational movement [2–6] imposed on the crystal and/or the crucible, which is opposed to natural convection [7–10]. We pass thus from the mode of dominating free

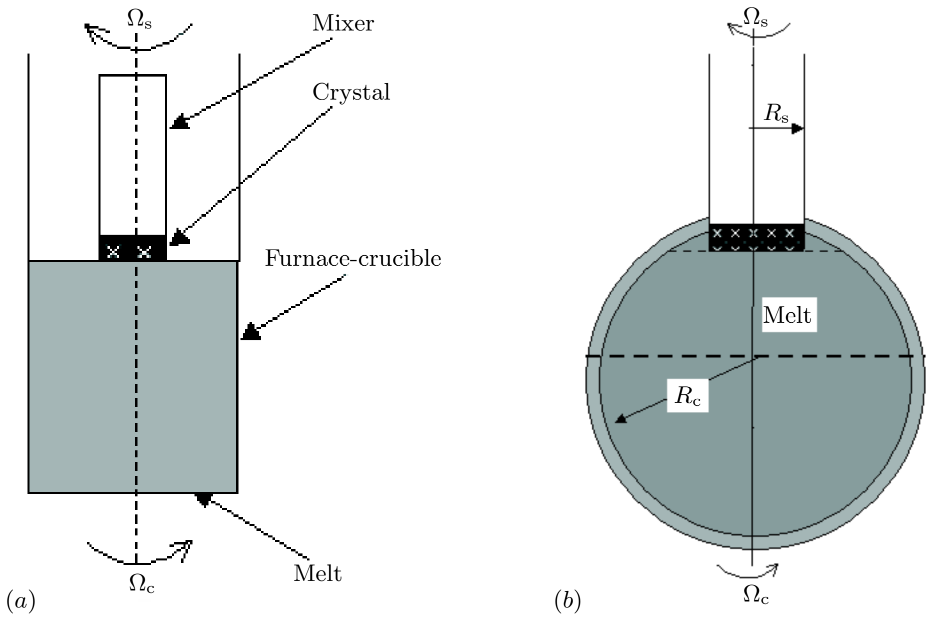

Fig. 1. (*a*) System cylinder/cylinder. (*b*) Alternative system cylinder/sphere.

convection to the mode of controlled forced convection. Other types of forces, as the magnetic field, can be used to attenuate the disturbances induced by the temperature [11, 12]. Flows generated by forces, which had gradients of surface stress [13–24], are also possible due to the crucible dimensions.

In addition, the quality of the produced crystal is influenced by the dynamics of the melt through the form of the liquid-solid interface, where latent heat of solidification is released, being able to generate thermal stresses responsible for the appearance of dislocation in the crystal.

1. Device. In the classical device, the molten material is placed in a cylindrical furnace crucible, at the fixed temperature T_c; the mixer, carrying the germ, is of the same cylinder center as the crucible (Fig. 1*a*). The two cylinders are moved by counter-rotating engines.

Anselmo *et al.* [25, 26] showed numerically that a crucible with a curved bottom has advantages for crystallization. It was taken into account in this observation that led us to replace the system cylinder/cylinder by a cylindrical-spherical system.

An alternative model is illustrated in Fig. 1*b*, which is called a cylindrical-spherical system, made up of a cylinder, carrying the germ of growth, of radius R_s. This cylinder rotates at an angular velocity Ω_s plunged in a spherical crucible, which contains a melt of silicon of radius R_c, temperature T_c, and is laid out on a table rotating with an angular velocity Ω_c.

2. Formulation of the problem. With account for the phenomenological complexity, one is motivated to make assumptions of simplification, namely:

- The thermophysical properties of the fluid are constant.
- The molten melt is a Newtonian and incompressible fluid and satisfies the Boussinesq approximation.

- The flow of the liquid within the crucible is laminar.
- The shape of the liquid-solid interface is supposed to be spherical.
- The system is axisymmetric.
- Calculations are carried out in a stationary mode.

The equations, governing the dynamics of the flow, result from the principles of conservation of mass and momentum, and the conservation equation of energy in the melt. The crucible has a spherical shape, therefore, we write our equations in spherical coordinates. V is the flow velocity, P is the associated pressure and T is the temperature, g is the field of gravity, Q is a source term coming from the radiation in the system.

Continuity

$$\frac{1}{r'^2}\frac{\partial}{\partial r}\left(r'^2 V'_r\right)+\frac{1}{r'\sin\theta}\frac{\partial}{\partial\theta}\left(V'_\theta\sin\theta\right)=0\,.$$

Momentum

$\mathbf{e}_r$:

$$V'_r\frac{\partial V'_r}{\partial r'}+\frac{V'_\theta}{r}\frac{\partial V'_r}{\partial\theta}-\frac{V'^2_\theta}{r}-\frac{V'^2_\varphi}{r}=-\beta g\big(T'-T_f\big)\cos\theta-\frac{1}{\rho}\frac{\partial P'}{\partial r}+$$

$$+\,\upsilon\cdot\left(\frac{1}{r'^2}\left[\frac{\partial}{\partial r'}\left(r'^2\frac{\partial V'_r}{\partial r'}\right)+\frac{1}{\sin\theta}\frac{\partial}{\partial\theta}\left(\sin\theta\frac{\partial V'_r}{\partial\theta}\right)\right]-\frac{2}{r^2}V'_r-\frac{2}{r'^2\sin\theta}\frac{\partial}{\partial\theta}\big(\sin\theta\cdot V'_\theta\big)\right).$$

$\mathbf{e}_\theta$:

$$V'_r\frac{\partial V'_\theta}{\partial r'}+\frac{V'_\theta V'_r}{r'}+\frac{V'_\theta}{r'}\frac{\partial V'_\theta}{\partial\theta}-\frac{V'^2_\varphi}{r}\cot\theta\quad=\beta g\left(T'-T_f\right)\sin\theta-\frac{1}{\rho}\frac{1}{r'}\frac{\partial P'}{\partial\theta}+$$

$$+\,\upsilon\cdot\left(\frac{1}{r'^2}\left[\frac{\partial}{\partial r'}\left(r'^2\frac{\partial V'_\theta}{\partial r'}\right)+\frac{1}{\sin\theta}\frac{\partial}{\partial\theta}\left(\sin\theta\frac{\partial V'_\theta}{\partial\theta}\right)\right]-\frac{1}{r'^2\sin^2\theta}V'_\theta+\frac{2}{r'^2}\frac{\partial V'_r}{\partial\theta}\right).$$

$\mathbf{e}_\varphi$:

$$V'_r\frac{\partial V'_\varphi}{\partial r'}+\frac{V'_\theta}{r'}\frac{\partial V'_\varphi}{\partial\theta}+\frac{V'_\theta V'_\varphi}{r'}\cot\theta+\frac{V'_r V'_\varphi}{r'}=$$

$$=\upsilon\cdot\left(\frac{1}{r'^2}\left[\frac{\partial}{\partial r'}\left(r'^2\frac{\partial V'_\varphi}{\partial r'}\right)+\frac{1}{\sin\theta}\frac{\partial}{\partial\theta}\left(\sin\theta\frac{\partial V'_\varphi}{\partial\theta}\right)\right]-\frac{1}{r'^2\sin^2\theta}V'_\varphi\right).$$

Energy

$$V'_r\frac{\partial T'}{\partial r'}+\frac{V'_\theta}{r}\frac{\partial T'}{\partial\theta}=\frac{\upsilon}{\alpha\cdot r'^2}\left[\frac{\partial}{\partial r'}\left(r'^2\frac{\partial T'}{\partial r'}\right)+\frac{1}{\sin\theta}\frac{\partial}{\partial\theta}\left(\sin\theta\frac{\partial T'}{\partial\theta}\right)\right]+Q'\,.$$

ρ is the density, μ is the dynamic viscosity and α is the molecular diffusivity of the fluid.

3. Boundary conditions.

Crucible wall:	$r'=R_\mathrm{c}$	$V=\Omega_\mathrm{c}R_\mathrm{c}\sin\theta.\mathrm{e}_\varphi$,		$T'=T_\mathrm{c}$
Crystal bottom:	$r=R_\mathrm{s}$	$V=\Omega_\mathrm{s}R_\mathrm{s}\sin\theta.\mathrm{e}_\varphi$,		$T'=T_\mathrm{f}$
Free surface:	$\theta=\frac{\pi}{2}$	$V'_\theta=0$	and	$\frac{\partial V'_\varphi}{\partial\theta}=0$

The use of the reduced variables makes it possible to closer approach the reality of the physical phenomena because their existences and evolutions are independent of the system of measuring units used to study them. One can also say that these variables make it possible to obtain general information, which plays a dominating role in the similarities. Indeed, to transform the phenomenologic equations in an adimensional form, it is necessary to define, realising characteristic sizes, changes of the variables.

Therefore, one calls upon the following reference variables: the length R_{c} – radius of the crucible, and the temperature T_{f} – melting temperature.

The reduced variables are then given by

$$r = \frac{r'}{R_{\mathrm{c}}}, \qquad V_r = \frac{V_r' R_{\mathrm{c}}}{\upsilon}, \qquad V_\theta = \frac{V_\theta' R_{\mathrm{c}}}{\upsilon}, \qquad V_\varphi = \frac{V_\varphi' R_{\mathrm{c}}}{\upsilon},$$
$$P = \frac{P' R_{\mathrm{c}}^2}{\rho \upsilon^2}, \qquad T = \frac{T' - T_{\mathrm{f}}}{T_{\mathrm{c}} - T_{\mathrm{f}}}, \qquad Q = \frac{Q' R_{\mathrm{c}}^2}{\rho \upsilon^2}\ .$$

The system of equations, which govern the problem, writes then in the following adimensional form:

Continuity

$$\frac{1}{r^2}\frac{\partial}{\partial r}\left(r^2 V_r\right) + \frac{1}{r\sin\theta}\frac{\partial}{\partial\theta}\left(V_\theta \sin\theta\right) = 0\ .$$

Momentum

$$V_r\frac{\partial V_r}{\partial r} + \frac{V_\theta}{r}\frac{\partial V_r}{\partial\theta} - \frac{V_\theta^2}{r} - \frac{V_\varphi^2}{r} = -\mathrm{Gr}\cdot T\cos\theta - \frac{\partial P}{\partial r} +$$
$$+\left(\frac{1}{r^2}\left[\frac{\partial}{\partial r}\left(r^2\frac{\partial V_r}{\partial r}\right) + \frac{1}{\sin\theta}\frac{\partial}{\partial\theta}\left(\sin\theta\frac{\partial V_r}{\partial\theta}\right)\right] - \frac{2}{r^2}V_r - \frac{2}{r^2\sin\theta}\frac{\partial}{\partial\theta}(\sin\theta\cdot V_\theta)\right)\ .$$

$$V_r\frac{\partial V_\theta}{\partial r} + \frac{V_\theta V_r}{r} + \frac{V_\theta}{r}\frac{\partial V_\theta}{\partial\theta} - \frac{V_\varphi^2}{r}\cot\theta \quad = \mathrm{Gr}\cdot T\sin\theta - \frac{1}{r}\frac{\partial P}{\partial\theta} +$$
$$+\left(\frac{1}{r^2}\left[\frac{\partial}{\partial r}\left(r^2\frac{\partial V_\theta}{\partial r}\right) + \frac{1}{\sin\theta}\frac{\partial}{\partial\theta}\left(\sin\theta\frac{\partial V_\theta}{\partial\theta}\right)\right] - \frac{1}{r^2\sin^2\theta}V_\theta + \frac{2}{r^2}\frac{\partial V_r}{\partial\theta}\right)\ .$$

$$V_r\frac{\partial V_\varphi}{\partial r} + \frac{V_\theta}{r}\frac{\partial V_\varphi}{\partial\theta} + \frac{V_\theta V_\varphi}{r}\cot\theta + \frac{V_r V_\varphi}{r} \quad =$$
$$= \left(\frac{1}{r^2}\left[\frac{\partial}{\partial r}\left(r^2\frac{\partial V_\varphi}{\partial r}\right) + \frac{1}{\sin\theta}\frac{\partial}{\partial\theta}\left(\sin\theta\frac{\partial V_\varphi}{\partial\theta}\right)\right] - \frac{1}{r^2\sin^2\theta}V_\varphi\right)\ .$$

Energy

$$V_r\frac{\partial T}{\partial r} + \frac{V_\theta}{r}\frac{\partial T}{\partial\theta} \quad = \frac{1}{\mathrm{Pr}}\left(\frac{1}{r^2}\left[\frac{\partial}{\partial r}\left(r^2\frac{\partial T}{\partial r}\right) + \frac{1}{\sin\theta}\frac{\partial}{\partial\theta}\left(\sin\theta\frac{\partial T}{\partial\theta}\right)\right]\right) + Q\ .$$

We eliminate the pressure from the first and second equations by deriving, and following θ and r, we get

$$\frac{\partial}{\partial\theta}\left(V_r\frac{\partial V_r}{\partial r} + \frac{V_\theta}{r}\frac{\partial V_r}{\partial\theta} - \frac{V_\theta^2}{r} - \frac{V_\varphi^2}{r}\right) - \frac{\partial}{\partial r}r\cdot\left(V_r\frac{\partial V_\theta}{\partial r} + \frac{V_\theta V_r}{r} + \frac{V_\theta}{r}\frac{\partial V_\theta}{\partial\theta} - \frac{V_\varphi^2}{r}\cot\theta\right) =$$
$$= -\,\mathrm{Gr}\cdot\left(\frac{\partial}{\partial\theta}(T\cos\theta) + \frac{\partial}{\partial r}(r\cdot T\sin\theta)\right) + \frac{\partial}{\partial\theta}\left(\frac{1}{r^2}\Big[\frac{\partial}{\partial r}\Big(r^2\frac{\partial V_\theta}{\partial r}\Big) +\right.$$
$$\left. + \frac{1}{\sin\theta}\frac{\partial}{\partial\theta}\Big(\sin\theta\frac{\partial V_r}{\partial\theta}\Big)\Big] - \frac{2}{r^2}V_r - \frac{2}{r^2\sin\theta}\frac{\partial}{\partial\theta}(\sin\theta\cdot V_\theta)\right) - \qquad (1)$$

$$-\frac{\partial}{\partial r}r.\left(\left(\frac{1}{r^2}\left[\frac{\partial}{\partial r}\left(r^2\frac{\partial V_\theta}{\partial r}\right)+\frac{1}{\sin\theta}\frac{\partial}{\partial\theta}\left(\sin\theta\frac{\partial V_\theta}{\partial\theta}\right)\right]-\frac{1}{r^2\sin^2\theta}V_\theta+\frac{2}{r^2}\frac{\partial V_r}{\partial\theta}\right)\right)$$

$$V_r\frac{\partial V_\varphi}{\partial r}+\frac{V_\theta}{r}\frac{\partial V_\varphi}{\partial\theta}+\frac{V_\theta V_\varphi}{r}\cot\theta+\frac{V_r V_\varphi}{r}=$$
$$=\left(\frac{1}{r^2}\left[\frac{\partial}{\partial r}\left(r^2\frac{\partial V_\varphi}{\partial r}\right)+\frac{1}{\sin\theta}\frac{\partial}{\partial\theta}\left(\sin\theta\frac{\partial V_\varphi}{\partial\theta}\right)\right]-\frac{1}{r^2\sin^2\theta}V_\varphi\right) \quad (2)$$

$$\frac{1}{r^2}\frac{\partial}{\partial r}\left(r^2V_r\right)+\frac{1}{r\sin\theta}\frac{\partial}{\partial\theta}\left(V_\theta\sin\theta\right)=0. \quad (3)$$

$$V_r\frac{\partial T}{\partial r}+\frac{V_\theta}{r}\frac{\partial T}{\partial\theta}=\frac{1}{\mathrm{Pr}}\left(\frac{1}{r^2}\left[\frac{\partial}{\partial r}\left(r^2\frac{\partial T}{\partial r}\right)+\frac{1}{\sin\theta}\frac{\partial}{\partial\theta}\left(\sin\theta\frac{\partial T}{\partial\theta}\right)\right]\right)+Q\ , \quad (4)$$

where Gr and Pr are the adimensional numbers defined as follows. The Grashof number $\mathrm{Gr}=g\beta R_{\mathrm{c}}^3(T_{\mathrm{c}}-T_{\mathrm{f}})/\upsilon^2$ characterizes the effect of natural convection. The Prandtl number $\mathrm{Pr}=\upsilon/\alpha$ characterizes the importance of thermal diffusivity compared to molecular diffusivity.

For this new system of equations the boundary conditions are as follows:

$$r=1 \qquad V=\mathrm{Re_c}\sin\theta\cdot \mathrm{e}_\varphi \qquad T=1,$$
$$r=A \qquad V=\mathrm{Re_s}\sin\theta\cdot \mathrm{e}_\varphi \qquad T=0,$$
$$\theta=\frac{\pi}{2} \qquad V_\theta=0 \qquad \frac{\partial V_\varphi}{\partial\theta}=0,$$

where $A=\mathrm{Re_s}/\mathrm{Re_c}$ is the radius ratio. $\mathrm{Re_c}$, $\mathrm{Re_s}$ are the Reynolds numbers associated with the crucible and the crystal defined as:

$$\mathrm{Re_c}=\frac{R_{\mathrm{c}}^2\,\Omega_{\mathrm{c}}}{\upsilon}\ ,\qquad \mathrm{Re_s}=\frac{R_{\mathrm{c}}R_{\mathrm{s}}\,\Omega_{\mathrm{s}}}{\upsilon}\ .$$

4. Method of resolution. We propose the expressions of velocity and temperature fields, which verify the boundary conditions in advance so that

$$V_r=\sum_n\alpha_n\left(r-1\right)^2\left(r-A\right)^2r^{n-1}f\left(\theta\right),$$
$$V_\theta=\sum_n\beta_n\left(r-1\right)\left(r-A\right)r^{n-1}\,\Phi\left(\theta\right),$$
$$V_\varphi=\sum_n\gamma_n\left(ar+\frac{b}{r^2}\right)r^{n-1}\,\psi\left(\theta\right),$$
$$T=\sum_n\delta_n\left(r-A\right)r^{n-1}\,\Theta\left(\theta\right)\ .$$

By applying the boundary conditions to the form of V_φ, we can have the form of $\psi(\theta)$, a and b

$$\psi(\theta)=\psi_0\sin\theta\ ,\qquad a=\frac{A^2\mathrm{Re_s}-\mathrm{Re_c}}{A^3-1}\ ,\qquad b=\frac{A^3\mathrm{Re_c}-A^2\mathrm{Re_s}}{A^3-1}\ .$$

According to the Galerkin method [27], we replace these expressions in the equations of continuity and momentum and multiplying by

$$W_m=\sum_m\left(ar+\frac{b}{r^2}\right)r^{m-1}$$

we integrate hereafter between A and 1.

5. First order approximation. The next step is to carry out an approximation of the order of $n = m = 1$ to have an estimation of the solution.

$$V_r = \alpha_1 (r-1)^2 (r-A)^2 f(\theta),$$
$$V_\theta = \beta_1 (r-1)(r-A)\Phi(\theta),$$
$$V_\varphi = \gamma_1 \left(ar + \frac{b}{r^2}\right)\psi(\theta),$$
$$T = \delta_1 (r-A)\Theta(\theta) \ .$$

By performing, equation (3) is simplified as

$$C_1 \cdot f + \frac{1}{\sin\theta}\frac{\partial}{\partial\theta}(\Phi\sin\theta) = 0 \ , \tag{5}$$

where $C_1 = \dfrac{\alpha_1}{\beta_1}\dfrac{I_1}{I_2}$ is a constant to be fixed later on. I_1 and I_2 are integral expressions and given by

$$I_1 = \int_A^1 \left(a + \frac{b}{r^3}\right)\frac{\mathrm{d}}{\mathrm{d}r}\left(r^2 (r-1)^2 (r-A)^2\right)\mathrm{d}r$$
$$I_2 = \int_A^1 \left(ar + \frac{b}{r^2}\right)(r-1)(r-A)\,\mathrm{d}r \ .$$

The same procedure is applied to equation (2)

$$\alpha_1 C_1 \frac{\partial}{\partial\theta}(\Phi\sin\theta)\cdot I_3 + 2\beta_1\Phi\cos\theta\cdot I_4 = 0 \ , \tag{6}$$

where I_3 and I_4 are integral expressions and given by

$$I_3 = \int_A^1 (r-1)^2(r-A)^2\left(ar + \frac{b}{r^2}\right)\left[a + \frac{b}{r^3} + \frac{\mathrm{d}}{\mathrm{d}r}\left(ar + \frac{b}{r^2}\right)\right]\mathrm{d}r$$
$$I_4 = \int_A^1 \frac{1}{r}(r-1)(r-A)\left[ar + \frac{b}{r^3}\right]^2\mathrm{d}r \ .$$

The solution of equation (6) gives the following expression

$$\Phi = \frac{C}{\sin\theta^{1+N}} \ ,$$

where $N = -2\dfrac{I_1}{I_2}\dfrac{I_4}{I_3}$ and C being a constant of integration to be determined from the boundary conditions.

We derive the expression of f from equation (5).

$$f = -C_1 C_2 N\frac{\cos\theta}{\sin\theta^{N+2}} \ .$$

By replacing the velocity expression in equation (1) and applying the Galerkin method once again, we obtain

$$\frac{\partial}{\partial\theta}(\Theta\cos\theta) + p\cdot\Theta + \frac{g(\theta)}{\sin\theta} = 0. \tag{7}$$

The solution of this equation yields

$$\Theta = \cos\theta^p \left(- \int_\theta \frac{g(\theta)}{\cos\theta^{p+1}} \mathrm{d}\theta' + \Theta_0 \right),$$

with Θ_0 being a constant to be defined starting from the boundary conditions, p denotes an integer number, and $g(\theta)$ is the function of α_1, β_1, γ_1, A related to Φ and its first, second and third derivatives.

6. Second order approximation. Now having an assessment of the solution of the first order, we try to pass to a higher order in order to possibly approach the real solution of the problem.

$$\begin{aligned}
V_r &= \left(\alpha_1 + \frac{\alpha_2}{r}\right)(r-1)^2 (r-A)^2 f(\theta)\,, \\
V_\theta &= \left(\beta_1 + \frac{\beta_2}{r}\right)(r-1)(r-A)\,\Phi(\theta)\,, \\
V_\varphi &= \left(\gamma_1 + \frac{\gamma_2}{r}\right)\left(ar + \frac{b}{r^2}\right)\sin\theta, \\
T &= \left(\delta_1 + \frac{\delta_2}{r}\right)(r-A)\,\Theta(\theta)\ .
\end{aligned}$$

While working with this type of distributions, one faces contradictions resulting in finding all the constants zero-valued (velocities and temperature). To avoid this difficulty, we choose the form of V_θ starting from mathematical considerations based on the equations of continuity and the properties of stream function:

$$V_\theta = \left(\beta_1 + \frac{\beta_2}{r} + \beta_3 \cdot r\right)(r-1)(r-A)\ \Phi(\theta)\ .$$

The stream function $\Psi(r,\theta)$ in the spherical coordinates in an axisymmetric approximation is given by the following expression [28]:

$$V_r = \frac{1}{r^2 \sin\theta} \frac{\partial\Psi}{\partial\theta}\ , \qquad V_\theta = -\frac{1}{r\sin\theta}\frac{\partial\Psi}{\partial r}\ .$$

We derive $\Psi(r,\theta)$ from the expression $V_\theta = -\frac{1}{r\sin\theta}\frac{\partial\Psi}{\partial r}$, then we obtain

$$\Psi(r,\theta) = -\sin\theta\cdot\Phi(\theta)\int\left(\beta_1 + \frac{\beta_2}{r} + \beta_3\cdot r\right) r\,(r-1)(r-A)\,\mathrm{d}r + g(\theta)\ ,$$

where $g(\theta)$ is a function to be defined thereafter.

We calculate V_r using the expression $V_r = \frac{1}{r^2\sin\theta}\frac{\partial\Psi}{\partial\theta}$ so that

$$V_r = -\frac{1}{\sin\theta}\frac{\partial}{\partial\theta}\sin\theta\cdot\Phi(\theta)\cdot\frac{1}{r^2}\int\left(\beta_1 + \frac{\beta_2}{r} + \beta_3\cdot r\right) r\,(r-1)(r-A)\,\mathrm{d}r + g'(\theta)\ .$$

7. Boundary conditions of the stream function. According to W.E. Langlois [29], the stream function must satisfy the following boundary conditions:

on the axis of symmetry	$\Psi(r,0) = 0;$
at the crucible wall	$\Psi(1,\theta) = 0;$

at the crystal/melt interface $\Psi(A,\theta)=0$;
at the free surface $\Psi(r,\frac{\pi}{2})=0$.

And the radial velocity must satisfy the following:

at the crucible wall $V_r(1,\theta)=0$;
at the crystal/melt interface $V_r(1,\theta)=0$.

By applying these boundary conditions and after having carried out intermediate calculations, we obtain

$$g(\theta)=0,\quad g'(\theta)=0,\quad g(0)=0,\quad g(\frac{\pi}{2})=0\,;$$
$$\beta_1=-3\frac{\beta_3}{5}\,(A+1)\,,\quad \beta_2=\frac{\beta_3}{5}\cdot A\,.$$

By replacing these constants in the expressions for velocity and stream function, we get

$$V_\theta=\frac{\beta_3}{5}\left(-3\,(A+1)+\frac{A}{r}+5r\right)(r-1)\,(r-A)\;\Phi\,(\theta)$$
$$V_r=-\frac{\beta_3}{5}\cdot\frac{1}{r}\,(r-1)^2\,(r-A)^2\,\frac{1}{\sin\theta}\frac{\partial}{\partial\theta}\sin\theta\cdot\Phi\,(\theta)$$
$$\Psi=-\frac{\beta_3}{5}\cdot r\cdot(r-1)^2\,(r-A)^2\cdot\sin\theta\cdot\Phi\,(\theta)\ .$$

Consequently, V_φ is given by the following relation

$$V_\varphi=\left(1+\frac{\gamma}{r}\right)\left(ar+\frac{b}{r^2}\right)\sin\theta\ .$$

Under these conditions, we intend to establish the expression of $\Phi(\theta)$, and according to the Galerkin method [27], by replacing these expressions in equation (4) and multiplying it by $W_2=\left(1+\frac{\gamma}{r}\right)\left(a'r+\frac{b'}{r^2}\right)$, we integrate thereafter between A and 1. We find that

$$\frac{\partial}{\partial\theta}\Big(\Phi\sin\theta\Big)+N_2\cdot\Phi\cos\theta=M_2\sin\theta\ , \tag{8}$$

where N_2 and M_2 are the constants given by $N_2=\frac{K_2}{K_1}$, $M_2=\frac{K_3}{K_1}$ and K_1, K_2 and K_3 are the integral expressions.

Equation (8) is a first order differential equation with a second term so that its solution yields

$$\Phi=\frac{1}{\sin\theta^{1+N_2}}\left(C_2+M_2\int\limits_{\theta}\sin\theta'^{1+N_2}\mathrm{d}\theta'\right)\ ,$$

with C_2 being a constant of integration to be defined from the boundary conditions. $\theta=\frac{\pi}{2}$, $V_\theta=0$, then $C_2=M_2\int_0^{\pi/2}\sin{\theta'}^{1+N_2}\mathrm{d}\theta'$, from where we obtain

$$\Phi=\frac{M_2}{\sin\theta^{1+N_2}}\left(\int\limits^{\theta}\sin{\theta'}^{1+N_2}\mathrm{d}\theta'-\int\limits_0^{\pi/2}\sin{\theta'}^{1+N_2}\mathrm{d}\theta'\right)\ .$$

Lastly, to find the temperature distribution, we replace the velocity expression in equation (1) and applying the Galerkin method once again we obtain the following equation

$$\frac{\partial}{\partial\theta}(\Theta\cos\theta) + p_2\cdot\Theta + \frac{g_2(\theta)}{\sin\theta} = 0\ , \tag{9}$$

where $g_2(\theta)$ is a function of Φ and its first, second and third derivative.

$$\Theta = \cos\theta^{p_2}\left(-\int\limits_{\theta}\frac{g_2(\theta)}{\cos\theta^{p_2+1}}\mathrm{d}\theta' + \Theta_2\right)$$

and Θ_2 denotes a constant to be defined from the boundary layer applied to θ.

8. Results and discussion. By applying the Galerkin method to order two, the number of constants doubled. As said previously, when we go up with a higher order, the optimization of these constants is in conformity with the physical sense of the phenomenon, requiring then the introduction of a parameter $K = 1 + N_2$, which relates all these constants.

The new expression of $\Phi(\theta)$ is the following

$$\Phi = \frac{M_2}{\sin\theta^K}\left(\int\limits^{\theta}\sin\theta'^K\mathrm{d}\theta' - \int\limits_0^{\pi/2}\sin\theta'^K\mathrm{d}\theta'\right)$$

and,

$$f = -\frac{M_2}{\sin\theta}\frac{\partial}{\partial\theta}\frac{1}{\sin\theta^{K-1}}\left(\int\limits^{\theta}\sin\theta'^K\mathrm{d}\theta' - \int\limits_0^{\pi/2}\sin\theta'^K\mathrm{d}\theta'\right).$$

And, finally, the expression of the stream function is

$$\Psi = -\frac{\beta_3}{5}r(r-1)^2(r-A)^2\frac{M_2}{\sin\theta^{K-1}}\left(\int\limits^{\theta}\sin\theta'^K\mathrm{d}\theta'\int\limits_0^{\pi/2}\sin\theta'^K\mathrm{d}\theta'\right).$$

By taking positive values of K, we note that the condition on the axis of symmetry, namely, the stream function, which is zero-valued, is not satisfied. The odd values of K lead to a problem of indetermination; but for negative pair values the preceding condition is satisfied and the functions obtained are well defined in the range of variation of the variable θ: $0 \le \theta \le \frac{\pi}{2}$.

In what follows, some values of K are given and velocities and corresponding stream functions are presented. Therefore, we study differents cases depending on the value of K.

8.1. Case $K = 0$. For this value, the velocities (ψ, Φ, f) and the stream function are given by

$$\psi = \sin\theta\ ,\quad \Phi = \theta - \frac{\pi}{2}\ ,\quad f = -\left(\theta - \frac{\pi}{2}\right)\cot\theta - 1\ ,$$
$$\Psi = \Psi_0 r\,(r-1)^2\,(r-A)^2\left(\theta - \frac{\pi}{2}\right)\sin\theta\ ,$$

introducing $\Psi = \Psi_1(r)\Psi_2(\theta)$, where Ψ_1 and Ψ_2 represent the radial and angular parts of the stream function.

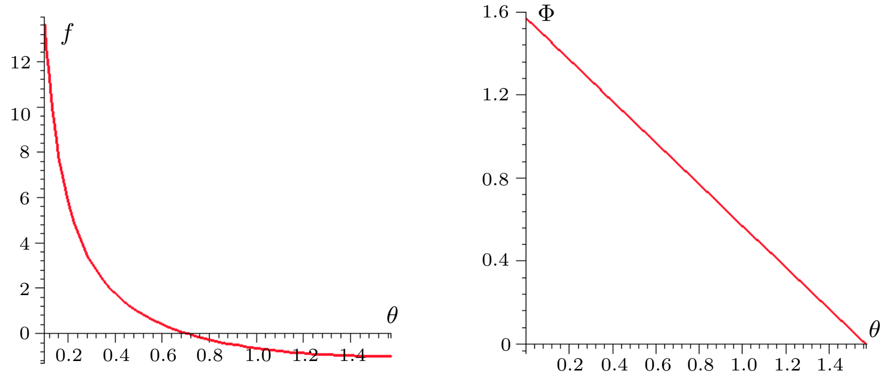

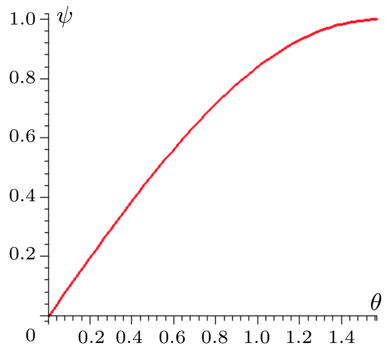

Fig. 2. Evolution of f, Φ and ψ with respect to θ for $K = 0$.

The streamlines obtained show that for this value of K (Fig. 4) there is only one structure corresponding to one bulk. This is very interesting for the quality of the grown crystal because the multiplicity of vortices or bulks suggests the appearance of the defects inside this one.

8.2. Case $K = -2$. For this value, the velocities (ψ, Φ, f) and the stream function Ψ are given by

$$\psi = \sin\theta\,, \quad \Phi = \sin\theta\cos\theta\,, \quad f = 2\cos^2\theta - \sin^2\theta\,,$$
$$\Psi = \Psi_0 r\,(r-1)^2\,(r-A)^2 \sin^2\theta\cos\theta\,,$$

where $\Psi_1 = r(r-1)^2(r-A)^2$ and $\Psi_2 = \sin^2\theta\cos\theta$.

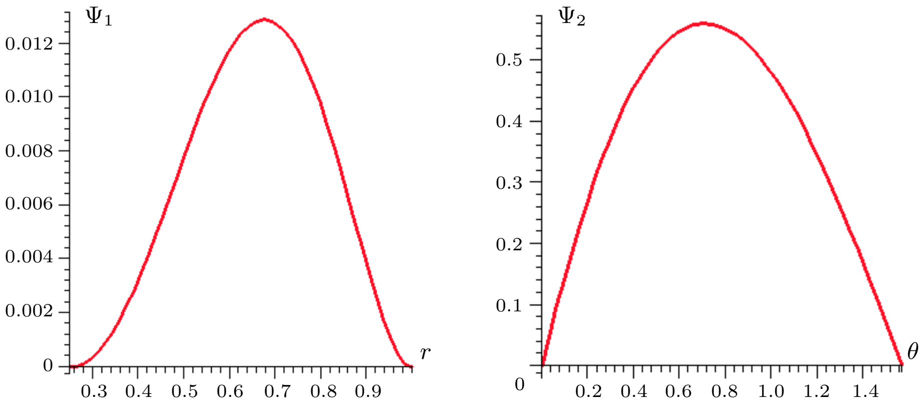

Fig. 3. Evolution of the radial and angular parts of the stream function with respect to r and θ for $K = 0$.

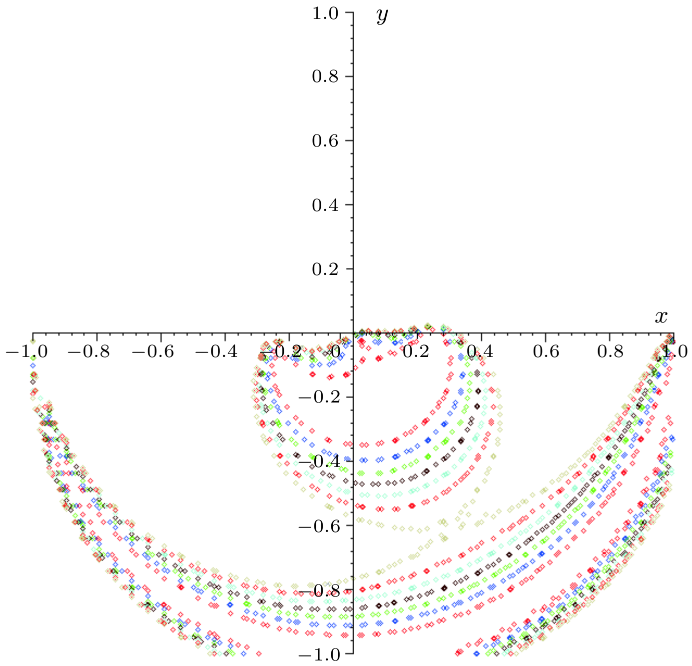

Fig. 4. Streamlines for $K = 0$.

By comparing the velocity profiles obtained for $K = 0$ (Fig. 2) and $K = -2$ (Fig. 5), we note that the evolution of f and Φ changes considerably, while that of ψ remains the same. The variation of Φ became parabolic and almost symmetric, whereas it was linear for $K = 0$, its maximum value is the third of that in the first

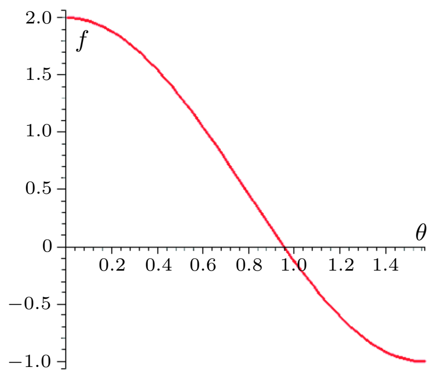

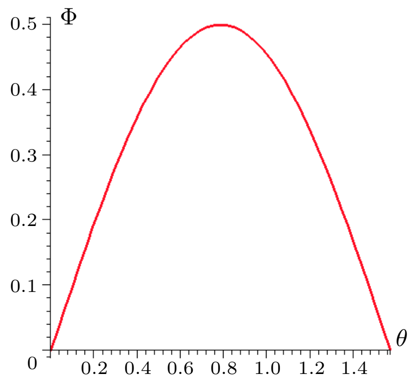

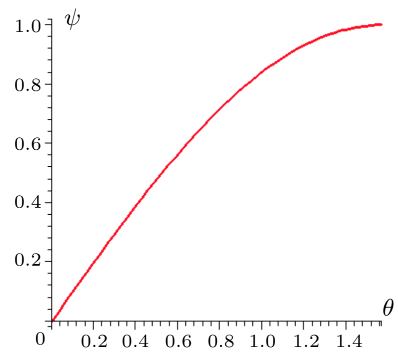

Fig. 5. Evolution of f, Φ and ψ with respect to θ for $K = -2$.

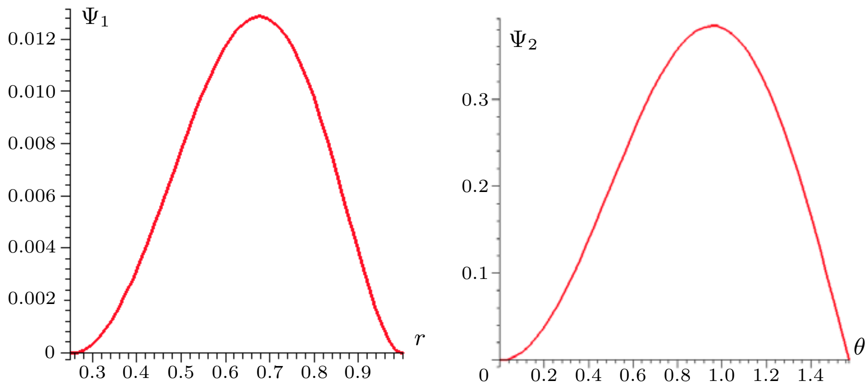

Fig. 6. Evolution of the radial and angular parts of the stream function with respect to r and θ for $K = -2$.

case (it changes from 1.5 to 0.5). For the radial velocity, we note that it starts to take more negative values, which reveal a point of inflection. We also deduce that its maximum value decreased from 14 to 2.

Analyzing the radial and angular parts of the stream function (Fig. 6), we note that their evolutions remain identical if compared to the first case (Fig. 3) but that of Ψ_2 loses its symmetry if compared to the origin. It flattened the free surface of the melt that corresponds to $\theta = \pi/2$. Its maximum changed from 0.57 to 0.39 for $\theta = 1$ rad. The structure of the streamlines (Fig. 7) changed considerably if compared to the first case (Fig. 4). We point out the formation of two symmetric structures at the axis of revolution. The transformation of only one structure for $K = 0$ versus two for $K = -2$ can explain the loss of symmetry of the angular part of the stream function and the appearance of a negative value corresponding to the radial velocity variations.

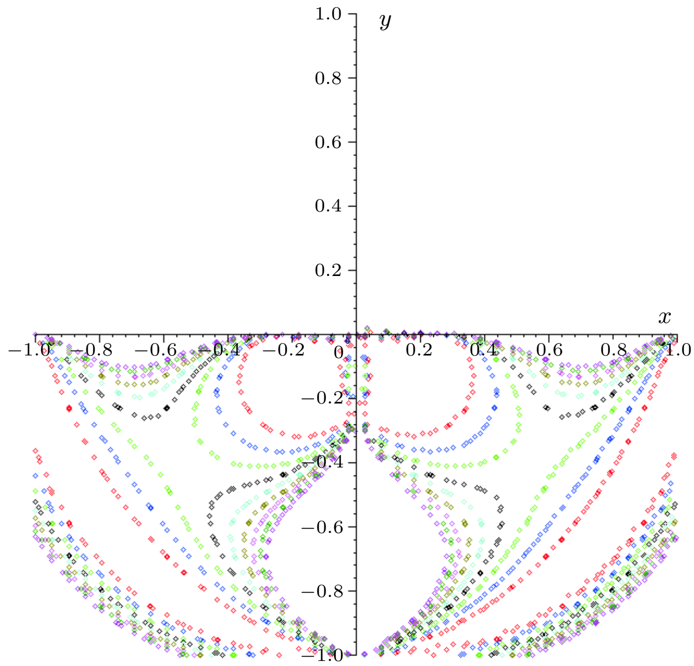

Fig. 7. Streamlines for $K = -2$.

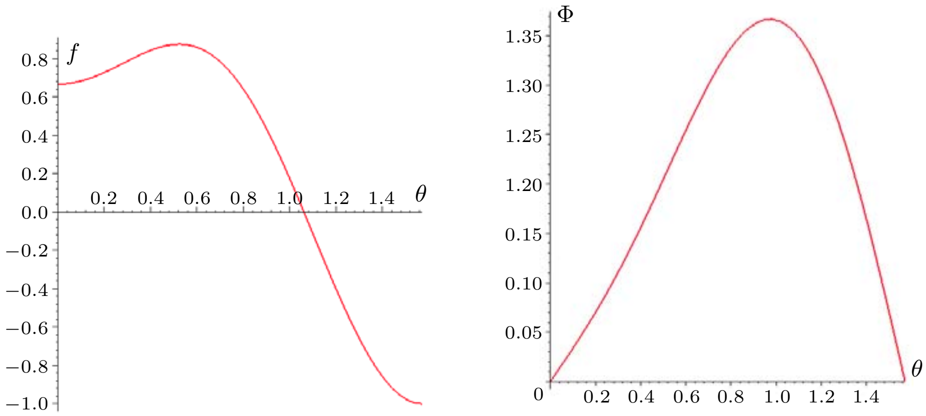

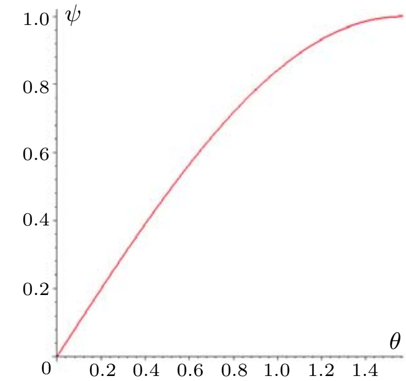

Fig. 8. Evolution of f, Φ and ψ with respect to θ for $K = -4$.

8.3. Case $K = -4$. For this value, the velocities and the stream function are given by

$$\psi = \sin\theta \,, \quad \Phi = \frac{1}{3}\sin^3\theta \cdot \cos\theta\,(\sin\theta + 2) \;, \quad f = -\frac{10}{3}\cos^4\theta + 5\cos^2\theta - 1 \,,$$
$$\Psi = \Psi_0 \cdot r\,(r-1)^2\,(r-A)^2 \cdot \frac{1}{3}\cos\theta \cdot \left(3 - 5\cos^2\theta + 2\cos^4\theta\right) \;,$$
$$\Psi_1 = r\,(r-1)^2\,(r-A)^2 \;, \quad \Psi_2 = \frac{1}{3}\cos\theta \cdot \left(3 - 5\cos^2\theta + 2\cos^4\theta\right) \;.$$

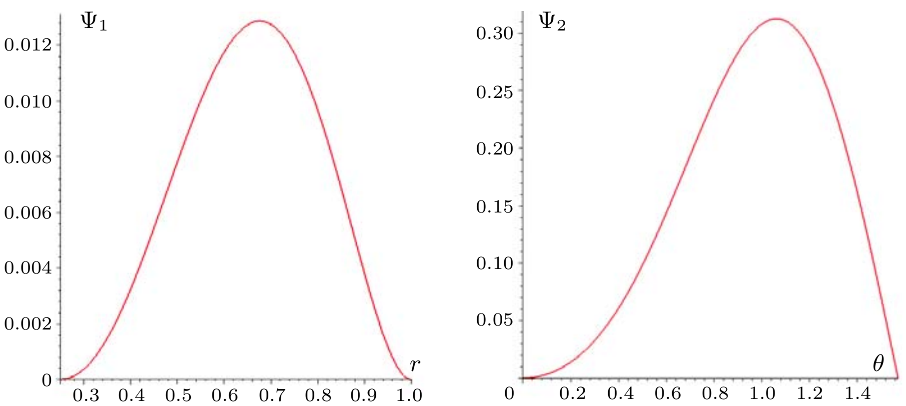

Fig. 9. Evolution of the radial and angular parts of the stream function with respect to r and θ for $K = -4$.

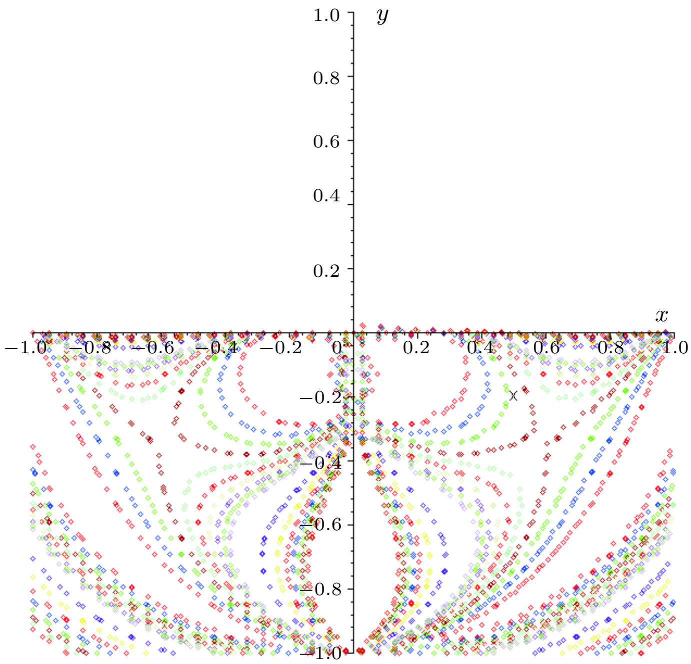

Fig. 10. Streamlines for $K = -4$.

Comparing the obtained velocity profils (Fig. 8) to the preceding case (Fig. 5) we note that Φ starts to lose its symmetry, its maximum value changes from 0.5 to 0.37 that corresponds to $\theta = 0.8$ rad and $\theta = 1.02$ rad, this one is flattened on the free surface. With regard to the angular part of the radial velocity, we note that it takes even more negative values, its minimal value is -1 for $\theta = \pi/2$ and its maximum value is 0.9 for $\theta = 0.56$ rad. The point of inflection moved from $\theta = 0.96$ rad for $K = -2$ to $\theta = \pi/2$ for $K = -4$. One also observes that the evolution of f between $\theta = 0.56$ rad and $\theta = \pi/2$ is strongly similar to its evolution between $\theta = 0$ and $\theta = \pi/2$ for $K = -2$. The profile of the angular part of the azimuthal velocity Ψ does not change at all if compared to the two preceding cases, in the same way for the radial part of the stream function.

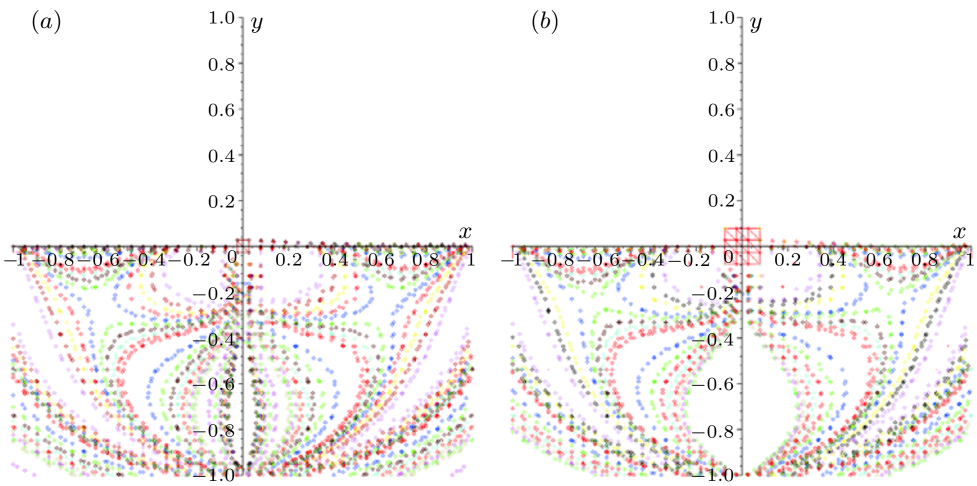

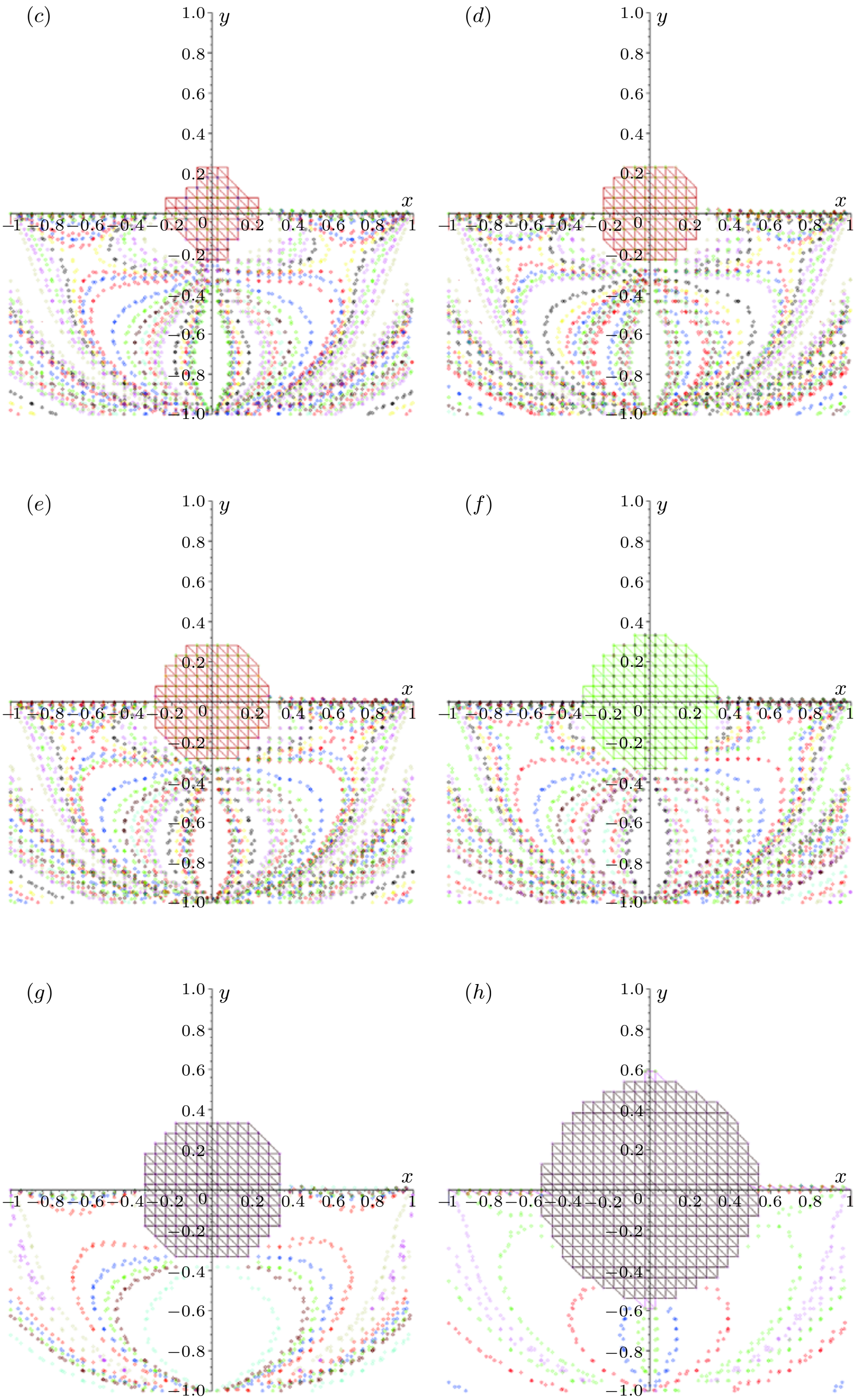

Fig. 11. Streamlines for: (a) $K = -8$, (b) $K = -10$, (c) $K = -12$, (d) $K = -14$, (e) $K = -16$, (f) $K = -18$, (g) $K = -20$ (h) $K = -30$.

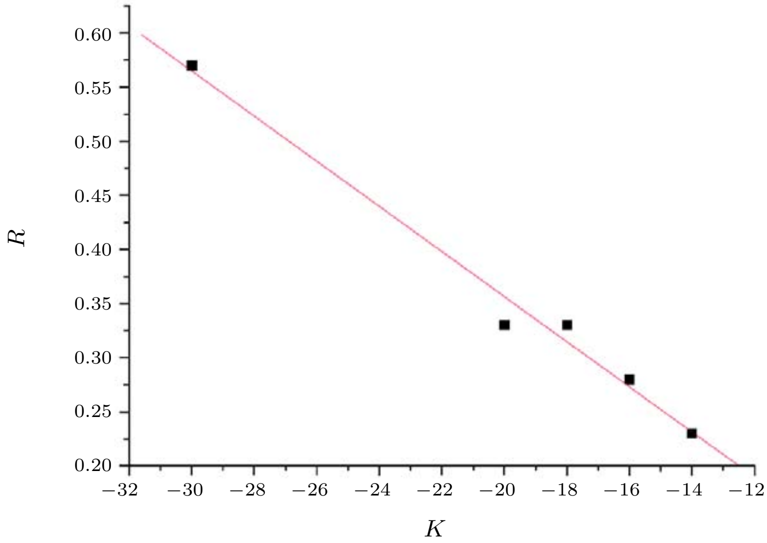

Fig. 12. Evolution of the spherical radius R due to the parameter K.

While analyzing the evolution of the angular part of the stream function, we note that it is flattened even more on the free surface (Fig. 9) and that its maximum value is shifted from 0.39 for $\theta = 1$ rad (Fig. 6) to 0.32 for $\theta = 1.06$ rad (Fig.9).

Analysis of the streamlines obtained (Fig. 10) shows that those are similar to the preceding case (Fig. 7). The analysis of the results, corresponding to $K = -10$ and $K = -12$, reveales a transitory behaviour of the transfromation of the cylindrical form into the spherical form. Consequently, the shaping parameter K reveals a critical state, which is a question of future research on the basis of the data of the velocity field associated with the temperature field.

Beyond the value of $K_{\mathrm{c}} = -12$ the tendency towards the spherical shape is reinforced considerably at $K = -30$. We note a remarkable property binding the adimensional radius of curvature of the sphere at the parameter K, which seems to be a control parameter of crystal growth. The data processing available in the studied interval $12 < -K < 30$ suggests a linear evolution of the form

$$10^2 R = 2.1\,(-K) - 6.1\ .$$

This relation can be exploited in practice to define in advance the spherical radius for the considered crystal.

Under the approximation conditions of the studied equations, it remains to continue our research beyond the value $K = -30$ to examine the coherence of our calculations for the obtained spherical form as well. In other words, up to which value of K can we consider the model to be stable? Moreover, a better smoothing of the obtained results is necessary to improve the representation of streamlines.

9. Conclusion. The modification of the Czochralski process according to the spherical shape of the crucible involves the change of the grown crystal conformation: it transfroms thus from the cylindrical to the spherical form.

Under these conditions the modified process then defines a new system presenting interesting characteristics of the flow: the sheared and counter-rotating motion with a high degree of symmetry presenting a great field of stability for the spherical shape of the grown crystal as well. The elaborate theoritical model made it possible to account for the physical reality of the results obtained through the analysis of the distribution of the velocity field and the representation of the corresponding streamlines, which primarily depend on the adimensional parameter K.

It is also remarkable to note that there is a simply linear relation between the curvature radius R of the crystal and the control parameter of the shape of crystal growth K.

This work deserves a deeper research to find out the field of validity associated with the parameter K in order to consider tests on an assured basis because we do not have theoretical or experimental results to our knowledge on this new type of process.

REFERENCES

[1] W.E. Langlois. *Ann. Rev. Fluid Mechanics*, vol. 17 (1985), pp. 191–215.

[2] G. Muller. *J. Crystal Growth.*, vol. 128 (1993), p. 26.

[3] S. Enger, B. Basu, M. Breuer, F. Durst. *J. Crystal Growth.*, vol. 219 (2000), p. 144.

[4] B. Basu, S. Enger, M. Breuer, F. Durst. *J. Crystal Growth.*, vol. 230 (2001), p. 148.

[5] Z. Galazka, D. Schwabe, H. Wilke. *Cryst. Res. Technol.*, vol. 38 (2003), p. 859.

[6] M.J. Crochet, P.J. Wouters. *J. Crystal Growth.*, vol. 65 (1983), p. 153.

[7] N. Kobayashi. *J. Crystal Growth.*, vol. 43 (1978), p. 357.

[8] W.E. Langlois. *J. Crystal Growth.*, vol. 46 (1979), p. 743.

[9] C. Milhelcic, Schroeck-Pauli, K. Wingerath. *J. Crystal Growth.*, vol. 57 (1982), p. 300.

[10] A. Bottaro, A. Zebib. *Phys. Fluids*, vol. 31 (1987), p. 495.

[11] K. Kakimoto, L. Liu. *Cryst. Res. Technol.*, vol. 38 (2003), p. 716.

[12] C. Milhelcic, Schroeck-Pauli, K. Wingerath. *J. Crystal Growth.*, vol. 71 (1985), p. 163.

[13] R. Rupp, G. Müller, G. Neumann. *J. Crystal Growth.*, vol. 97 (1989), p. 34.

[14] K. Kakimoto. *Prog. Crystal Growth Charact.*, vol. 30 (1995), p. 191.

[15] K. Kakimoto M. Wanatabe, E. Eguchi, T. Hibiya. *J. Crystal Growth.*, vol. 126 (1993), p. 435.

[16] K. Kakimoto, H. Ozoe. *J. Crystal Growth*, vol. 212 (2000), p. 429.

[17] M. Li, Y. Li, N. Imaishi. *J. Crystal Growth.*, vol. 234 (2002), p. 32.

[18] H. Nakanishi, M. Wantabe, K. Terashima. *J. Crystal Growth.*, vol. 236 (2002), no. 4, p. 523.

[19] K. Yi, K. Kakimoto, M. Eguchi, M. Watanabe, T. Shyo, T. Hibiya. *J. Crystal Growth.*, vol. 144 (1994), p. 20.

[20] V. Kumar, B. Basu, S. Enger, G. Brenner, F. Durst. *J. Crystal Growth.*, vol. 253 (2003), p. 142.

[21] S. Enger, O. Grabner, G. Muller, M. Breuer, F. Durst. *Phys. Fluids*, vol. 230 (2001), p. 135.

[22] V. Kumar, B. Basu, S. Enger, G. Brenner, F. Durst. *J. Crystal Growth.*, vol. 255 (2003), p. 27.

[23] H. Nakanishi, M. Watanabe, K. Terashima. *J. Crystal Growth.*, vol. 236 (2002), p. 523.

[24] F. Mokhtari, A. Bouabdallah, S. Hanchi, M. Zizi. *Algerian Journal of Technology*, April (2005), pp. 223–229.

[25] A.P. Anselmo, V. Prasad. *Prog. Crystal Growth Charact.*, vol. 134 (1993), pp. 116–139.

[26] A.P. Anselmo, V. Prasad. *J. Crystal Growth.*, vol. 131 (1993), pp. 247–264.

[27] A. Bouabdallah. Doctorates Science, Institut Polytechnique de Loraine/ Nancy, France, 1980.

[28] Chia-Shun Yih. *Fluid Mechanics* (McGraw-Hill Book Company, 1969).

[29] W.E. Langlois. *J. Crystal Growth.*, vol. 42 (1977), p. 386.

Received 01.02.2006